

**A comparative evaluation of the mechanical and surface properties of reinforced 3D printed polymethylmethacrylate and CAD CAM polymethylmethacrylate - An in-vitro study**

<sup>1</sup>Vinitha S Kumar, Postgraduate, Department of Prosthodontics and Crown and Bridge, Vokkaligara Sangha Dental College and Hospital, Rajiv Gandhi University of Health Sciences (RGUHS), Bengaluru, India.

<sup>2</sup>Archana Shetty, Reader, Department of Prosthodontics and Crown and Bridge, Vokkaligara Sangha Dental College and Hospital, Rajiv Gandhi University of Health Sciences (RGUHS), Bengaluru, India.

<sup>3</sup>Surendra Kumar G.P, Professor and Head, Department of Prosthodontics and Crown and Bridge, Vokkaligara Sangha Dental College and Hospital, Rajiv Gandhi University of Health Sciences (RGUHS), Bengaluru, India.

<sup>4</sup>Anupama N M, Professor, Department of Prosthodontics and Crown and Bridge, Vokkaligara Sangha Dental College and Hospital, Rajiv Gandhi University of Health Sciences (RGUHS), Bengaluru, India

<sup>5</sup>Jnanadev K R, Professor, Department of Prosthodontics and Crown and Bridge, Vokkaligara Sangha Dental College and Hospital, Rajiv Gandhi University of Health Sciences (RGUHS), Bengaluru, India

**Corresponding Author:** Vinitha S Kumar, Postgraduate, Department of Prosthodontics and Crown and Bridge, Vokkaligara Sangha Dental College and Hospital, Rajiv Gandhi University of Health Sciences (RGUHS), Bengaluru, India.

**Citation of this Article:** Vinitha S Kumar, Archana Shetty, Surendra Kumar G.P, Anupama N M, Jnanadev K R, “A comparative evaluation of the mechanical and surface properties of reinforced 3D printed polymethylmethacrylate and CAD CAM polymethylmethacrylate - An in-vitro study”, IJDSIR- November – 2025, Volume – 8, Issue – 6, P. No. 99 – 110.

**Copyright:** © 2025, Vinitha S Kumar, et al. This is an open access journal and article distributed under the terms of the creative common’s attribution non-commercial License. Which allows others to remix, tweak, and build upon the work non-commercially, as long as appropriate credit is given, and the new creations are licensed under the identical terms.

**Type of Publication:** Original Research Article

**Conflicts of Interest:** Nil

**Abstract**

**Introduction:** Polymethylmethacrylate (PMMA) denture bases fabricated through 3D printing technology are proven to be better in comparison to its digital counterpart, the subtractive CAD CAM technique, in terms of cost effectiveness, reduced wastage, better detail reproduction and ability to print complex geometries. However, the mechanical and surface properties of 3D printed denture bases are found to be inferior to both

conventional and CAD CAM techniques. Therefore, it is necessary to enhance the properties of 3D printed PMMA resin to make it a viable alternative to conventional and CAD CAM techniques.

**Aim:** To compare and evaluate the mechanical and surface properties of reinforced 3D printed PMMA with CAD CAM PMMA.

**Method:** A total of 72 samples of dimensions 64x10x3.3mm were divided into 4 groups (n=18), Group

I CAD CAM PMMA, Group II unmodified 3D printed PMMA, Group III 1wt% Al<sub>2</sub>O<sub>3</sub> reinforced 3D printed PMMA and Group IV 2.5wt% ZrO<sub>2</sub> reinforced 3D printed PMMA. Immediate flexural strength, surface hardness and surface roughness were tested after immersion in distilled water for 24 hours. Delayed flexural strength, surface hardness and surface roughness were tested after immersion in artificial saliva for 30 days followed by 5000 cycles of thermocycling simulating 6 months of intraoral use.

**Results:** The statistical analysis was performed using Kruskal-Wallis test and Wilcoxon signed-rank with significance set at p value < 0.05. Statistically significant differences (p < 0.05) were found among all groups. CAD CAM PMMA (Group I) had the highest immediate (116.20 ± 1.28 MPa) and delayed (108.25 ± 0.98 MPa) flexural strength, hardness (24.38 ± 0.64 VHN immediate; 22.82 ± 0.33 VHN delayed), and lowest roughness (0.66 ± 0.02 µm immediate; 0.74 ± 0.02 µm delayed). Zirconium oxide reinforcement (Group IV) showed higher flexural strength than Aluminum oxide (Group III), whereas Aluminum oxide reinforcement yielded the lowest surface roughness among the 3D printed groups.

**Conclusion:** Reinforcing 3D printed PMMA denture base resin with 2.5 wt% aluminum oxide or 1 wt% zirconium oxide significantly improved its mechanical and surface properties. While CAD-CAM PMMA remains superior, nanoparticle reinforcement offers a viable path to enhance the clinical performance of 3D printed resins.

**Keywords:** 3D printed PMMA, nanoparticles, Zirconium oxide, Aluminium oxide

### Introduction

The increase in life expectancy has led to a rise in the geriatric population, with edentulism being a prevalent

oral health problem.<sup>1</sup> Edentulous patients face functional, esthetic, and psychosocial challenges, and complete denture rehabilitation remains the most common treatment modality. The success of complete dentures depends on patient factors, the choice of material, and the fabrication method.<sup>2</sup>

Polymethylmethacrylate (PMMA), introduced by Walter Wright in 1936, has been the material of choice for denture base fabrication due to its favorable mechanical, physical, and esthetic properties. Conventional heat polymerization techniques such as compression molding and injection molding are widely used but have drawbacks such as porosity, polymerization shrinkage, surface roughness, and processing errors.<sup>1,3</sup>

Advancements in digital dentistry have introduced CAD CAM and 3D printing technologies for denture fabrication. CAD CAM milling uses pre-polymerized PMMA blanks fabricated under high temperature and pressure, providing superior mechanical and surface properties with minimal porosity and reduced microbial adhesion. However, the subtractive method involves significant material wastage and high fabrication costs.<sup>4,5</sup> 3D printing, an additive manufacturing technique, offers advantages such as reduced material waste, lower cost, faster production, and the ability to produce complex geometries. Nevertheless, 3D printed PMMA resins exhibit inferior mechanical and surface properties compared to conventional and CAD CAM PMMA.<sup>4,5</sup> Reinforcement of heat cured PMMA with metal oxides nanoparticles has been shown to improve the mechanical, surface, and antimicrobial properties.<sup>6</sup>

Limited literature exists on nanoparticle reinforcement of 3D printed PMMA denture base resins. This study aims to evaluate and compare the immediate and delayed mechanical and surface properties of reinforced 3D printed PMMA with CAD CAM PMMA

## Materials and Methodology

A total of 72 samples of dimensions 64x10x3.3mm were digitally designed and divided into 4 groups (n=18)

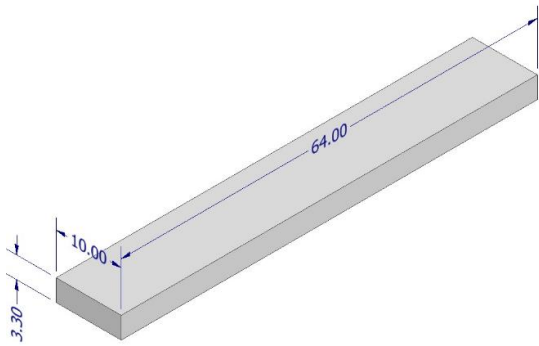


Figure 1: STL file of sample design

- **Group I:** CAD CAM PMMA
- **Group II:** Unmodified 3D printed PMMA
- **Group III:** 2.5 wt% Aluminum oxide–reinforced 3D printed PMMA
- **Group IV:** 1 wt% Zirconium oxide–reinforced 3D printed PMMA

## Specimen Preparation

**Group I- CAD CAM specimen preparation:** 18 CADCAM specimen were designed in the dimensions of (64 × 10 × 3.3mm) and milled to be tested for flexural strength, surface hardness and surface roughness. The specimens were cleaned using isopropyl alcohol bath with 99% purity for 10 minutes.



Figure 2: CAD CAM specimen preparation

## Group II- Unmodified 3D printed PMMA specimen

**preparation:** 18 unmodified 3D printed PMMA specimen with dimensions of (64 × 10 × 3.3 mm) were printed at 90° orientation to be tested for flexural strength, surface hardness and surface roughness. The 3D printing process was followed by thorough washing of specimens in an isopropyl alcohol bath with 99% purity for 10 minutes.



Figure 3: Unmodified 3D printed PMMA specimen preparation

## Group III- 2.5wt% Aluminium oxide nanoparticles reinforced 3D printed PMMA preparation:

Nanocomposite was prepared by gradual incorporation of 2.5wt% of Al<sub>3</sub>O<sub>2</sub> nanoparticles into the 3D printed PMMA solution under continuous magnetic stirring (Remi 1 MLH) for 30 minutes followed by mechanical mixing for 30 minutes at low frequency. The resultant resin was then used to print 18 aluminium oxide reinforced 3D printed PMMA specimen with dimensions of (64 × 10 × 3.3 mm) at 90° orientation to be tested for flexural strength, surface hardness and surface roughness. The 3D printing process was followed by thorough washing of specimens in an isopropyl alcohol bath with 99% purity for 10 minutes



Figure 4: 2.5wt% Aluminium oxide nanoparticles reinforced 3D printed PMMA preparation

**GROUP IV- 1wt% Zirconium oxide nanoparticles reinforced 3D printed PMMA preparation:**

Nanocomposite was prepared by gradual incorporation of 1wt% of ZrO<sub>2</sub> nanoparticles into the 3D printed PMMA solution under continuous magnetic stirring (Remi 1 MLH) for 30 minutes followed by mechanical mixing for 30 minutes at low frequency. The resultant resin was then used to print 18 zirconium oxide reinforced 3D printed PMMA specimen with dimensions of (64 × 10 × 3.3 mm) at 90o orientation to be tested for flexural strength, surface hardness and surface roughness. The 3D printing process was followed by thorough washing of specimens in an isopropyl alcohol bath with 99% purity for 10 minutes.



Figure 5: 1wt% Zirconium oxide nanoparticles reinforced 3D printed PMMA preparation

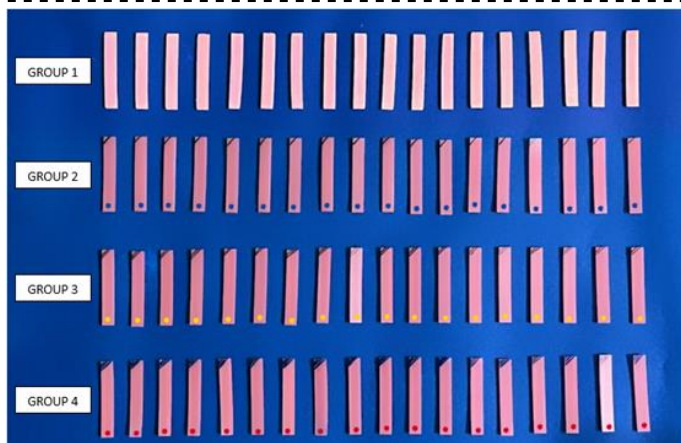


Figure 6: Samples categorized into respective groups

**Artificial ageing:** Twelve specimen from each group were stored in artificial saliva at 37°C for 30 days and subjected to thermocycling for 5000 cycles between 5°C to 55°C with dwell time of 30 seconds each, equivalent to 6 months of intraoral exposure.



Figure 7: Storage in artificial saliva for delayed testing



Figure 8: Thermocycling of samples for delayed testing

**Testing for flexural strength:** A three-point bending test was used to evaluate the flexural strength. The load was applied at the centre of the specimen until fracture. The fracture load (N) was recorded to calculate the flexural strength (MPa) using the equation  $FS = \frac{3Fl}{2bh^2}$ , where F= fracture load, l= length of specimen, b= width of the specimen and h= thickness of the specimen

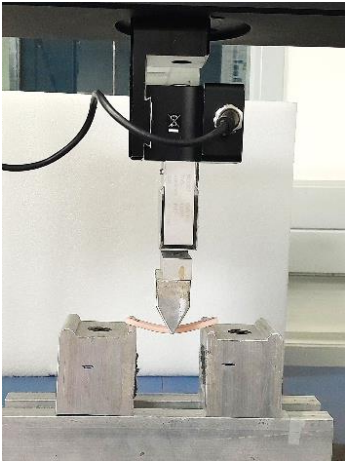


Figure 9: 3-point bending test for flexural strength using universal testing machine

**Testing for surface hardness:** Hardness was measured by Vickers hardness test and each specimen was subjected to a 50 N of load on three different sites. The final hardness (VHN) value of each specimen was arithmetically calculated by obtaining the average of the three readings.

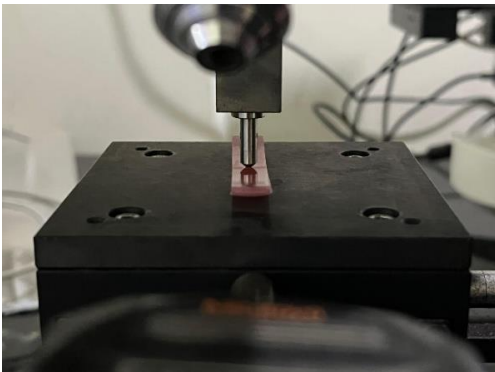


Figure 10: Vickers Hardness test for surface hardness

**Testing for surface roughness:** A non-contact optical profilometer was used for the measurement of the specimens' surface roughness. The specimens were radially scanned 3 times at different points with 0.01 mm resolution and the average surface roughness ( $\mu\text{m}$ ) for each specimen was calculated.

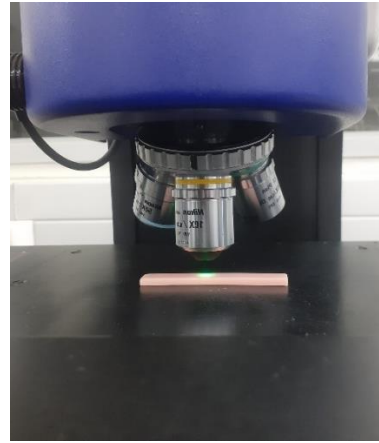


Figure 11: Non optical profilometer test for surface roughness

**Statistical analysis:** All statistical analyses were performed using IBM SPSS Statistics for Windows, Version 20.0 (IBM Corp., Armonk, NY, USA). Descriptive statistics were utilized to summarize quantitative data, with continuous variables expressed as means and standard deviations (SD) or medians with interquartile ranges (IQR), based on data distribution as assessed by the Shapiro-Wilk test. For intergroup comparisons of flexural strength, hardness, and roughness at both immediate and delayed time points, the Kruskal-Wallis test was employed owing to non-parametric data distribution, followed by pairwise comparisons using the Mann-Whitney U test with Bonferroni correction to control for type I error. The differences between immediate and delayed values within each group were analyzed using the Wilcoxon Signed-Rank test to determine the effect of artificial aging and thermocycling on material performance. A p-value of less than 0.05 was considered statistically significant.

**Results**

Table 1: Overall comparison of immediate flexural strength among the study groups

Groups	Mean±SD	Median (IQR)	Range	Chi-Square value; P value
Group 1	116.20±1.28	115.85 (115.13-117.40)	114.90-118.30	21.60; 0.001*
Group 2	86.33±1.22	86.30 (85.25-87.40)	84.80-88.00	
Group 3	98.63±0.99	98.45 (97.82-99.40)	97.60-100.30	
Group 4	104.17±0.93	104.25 (103.32-105.05)	102.80-105.20	

Kruskal Wallis test; \*statistically significant (p<0.05)

Table 2: Overall Comparison of delayed flexural strength among the study groups

Groups	Mean±SD	Median (IQR)	Range	Chi-Square value; P value
Group 1	108.25±0.98	108.50 (107.30-109.12)	106.70-109.20	21.60; 0.001*
Group 2	76.80±0.89	76.75 (75.95-77.62)	75.80-78.00	
Group 3	91.77±0.42	91.80 (91.40-92.07)	91.10-92.30	
Group 4	98.35±1.01	98.60 (97.17-99.15)	97.10-99.60	

Kruskal Wallis test; \*statistically significant (p<0.05)

Table 3: Comparison of immediate and delayed flexural strength

Groups	Immediate flexural strength	Delayed flexural strength	Z value; P value
Group 1	116.20±1.28	108.25±0.98	2.201; 0.028*
Group 2	86.33±1.22	76.80±0.89	2.207; 0.027*
Group 3	98.63±0.99	91.77±0.42	2.201; 0.028*
Group 4	104.17±0.93	98.35±1.01	2.207; 0.027*

Wilcoxon Signed Ranks test; \*statistically significant (p<0.05)

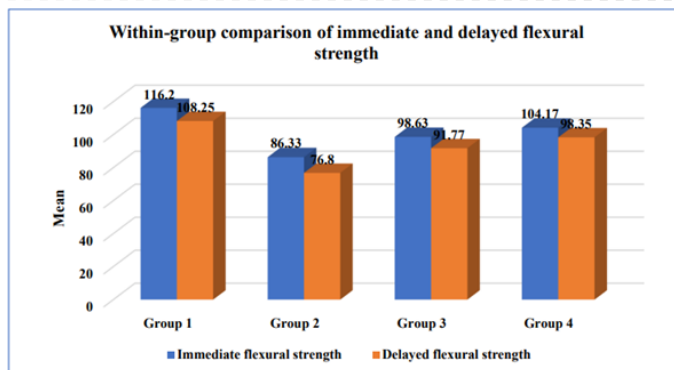


Figure 12: Within-group comparison of immediate and delayed flexural strength

CAD CAM PMMA (Group 1) showed the highest immediate flexural strength (116.20 ± 1.28 MPa), followed by ZrO<sub>2</sub> reinforced 3D-printed PMMA (Group 4, 104.17 ± 0.93 MPa), Al<sub>2</sub>O<sub>3</sub> reinforced 3D-printed PMMA (Group 3, 98.63 ± 0.99 MPa), and unmodified 3D-printed PMMA (Group 2, 86.33 ± 1.22 MPa) as the lowest.

After aging, flexural strength decreased in all groups. CAD CAM PMMA (Group 1) remained highest (108.25 ± 0.98 MPa), followed by ZrO<sub>2</sub> reinforced (Group 4, 98.35 ± 1.01 MPa), Al<sub>2</sub>O<sub>3</sub> reinforced (Group 3, 91.77 ± 0.42 MPa), and unmodified 3D-printed PMMA (Group 2, 76.80 ± 0.89 MPa).

Table 4: Overall comparison of immediate surface hardness among the study groups

Groups	Mean±SD	Median (IQR)	Range	Chi-Square value; P value
Group 1	24.38±0.64	24.40 (23.75-24.97)	23.60-25.20	20.95; 0.001*
Group 2	17.50±0.41	17.45 (17.20-17.87)	16.90-18.10	
Group 3	19.92±0.29	19.95 (19.65-20.15)	19.50-20.30	
Group 4	20.40±0.24	20.40 (20.17-20.62)	20.10-20.70	

Kruskal Wallis test; \*statistically significant (p<0.05)

Table 5: Overall comparison of delayed surface hardness between the study groups

Groups	Mean±SD	Median (IQR)	Range	Chi-Square value; P value
Group 1	22.82±0.33	22.75 (22.50-23.15)	22.40-23.30	19.71; 0.001*
Group 2	16.15±0.19	16.15 (15.97-16.32)	15.90-16.40	
Group 3	18.95±0.33	18.85 (18.67-19.32)	18.60-19.40	
Group 4	19.08±0.15	19.05 (18.97-19.22)	18.90-19.30	

Kruskal Wallis test; \*statistically significant (p<0.05)

Table 6: Comparison of immediate and delayed surface hardness

Groups	Immediate surface hardness	Delayed surface hardness	Z value; P value
Group 1	24.38±0.64	22.82±0.33	2.214; 0.027*
Group 2	17.50±0.41	16.15±0.19	2.201; 0.028*
Group 3	19.92±0.29	18.95±0.33	2.201; 0.028*
Group 4	20.40±0.24	19.08±0.15	2.201; 0.028*

Wilcoxon Signed Ranks test; \*statistically significant (p<0.05)

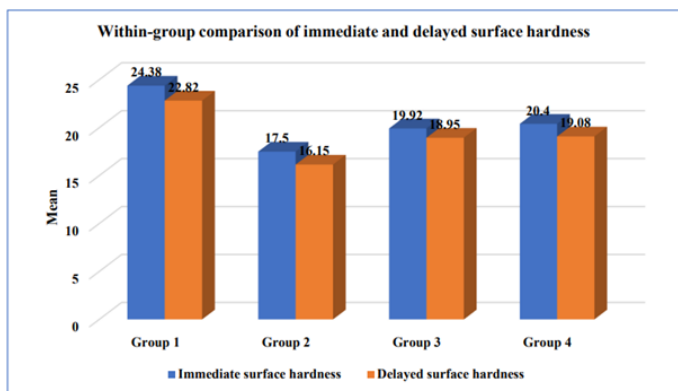


Figure 13: Within-group comparison of immediate and delayed surface hardness

For immediate hardness, CAD CAM PMMA (Group 1) recorded the highest mean value (24.38 ± 0.64 VHN), followed by ZrO<sub>2</sub> reinforced 3D-printed PMMA (Group 4, 20.40 ± 0.24 VHN), Al<sub>2</sub>O<sub>3</sub> reinforced PMMA (Group 3, 19.92 ± 0.29 VHN), and unmodified 3D-printed PMMA (Group 2, 17.50 ± 0.41 VHN) as the lowest.

After thermocycling, all groups showed a decrease in hardness. CAD CAM PMMA (Group 1) remained hardest (22.82 ± 0.33 VHN), followed by ZrO<sub>2</sub> reinforced (Group 4, 19.08 ± 0.41 VHN), Al<sub>2</sub>O<sub>3</sub> reinforced (Group 3, 18.95 ± 0.25 VHN), and unmodified 3D-printed PMMA (Group 2, 16.15 ± 0.19 VHN).

Table 7: Overall Comparison of immediate surface roughness among the study groups

Groups	Mean±SD	Median (IQR)	Range	Chi-Square value; P value
Group 1	0.66±0.02	0.65 (0.64-0.67)	0.63-0.68	16.28; 0.001*
Group 2	0.92±0.01	0.91 (0.91-0.93)	0.90-0.94	
Group 3	0.91±0.02	0.91 (0.88-0.92)	0.88-0.93	
Group 4	0.93±0.01	0.93 (0.92-0.94)	0.91-0.95	

Kruskal Wallis test; \*statistically significant (p<0.05)

Table 8: Overall comparison of delayed surface roughness among the study groups

Groups	Mean±SD	Median (IQR)	Range	Chi-Square value; P value
Group 1	0.74±0.02	0.73 (0.72-0.75)	0.71-0.76	20.96; 0.001*
Group 2	1.06±0.02	1.05 (1.03-1.07)	1.03-1.08	
Group 3	0.94±0.02	0.94 (0.91-0.95)	0.91-0.96	
Group 4	1.01±0.03	1.01 (0.98-1.03)	0.97-1.05	

Kruskal Wallis test; \*statistically significant (p<0.05)

Table 9: Comparison of immediate and delayed surface roughness

Groups	Immediate surface roughness	Delayed surface roughness	P value
Group 1	0.66±0.02	0.74±0.02	2.207; 0.027*
Group 2	0.92±0.01	1.06±0.02	2.220; 0.026*
Group 3	0.91±0.02	0.94±0.02	1.841; 0.066
Group 4	0.93±0.01	1.01±0.03	2.214; 0.027*

Wilcoxon Signed Ranks test; \*statistically significant (p<0.05)

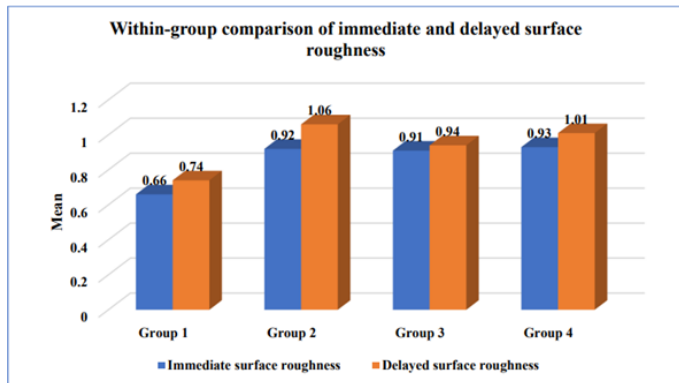


Figure 14: Within-group comparison of immediate and delayed surface hardness

Immediately after fabrication, CAD CAM PMMA (Group 1) showed the least surface roughness ( $0.66 \pm 0.02 \mu\text{m}$ ), followed by  $\text{Al}_2\text{O}_3$  reinforced 3D-printed PMMA (Group 3,  $0.91 \pm 0.02 \mu\text{m}$ ),  $\text{ZrO}_2$  reinforced (Group 4,  $0.93 \pm 0.01 \mu\text{m}$ ), and unmodified 3D-printed PMMA (Group 2,  $0.92 \pm 0.01 \mu\text{m}$ ) exhibited the highest surface roughness.

After aging, surface roughness increased for all groups. However, CAD CAM PMMA (Group 1) still exhibited the lowest surface roughness ( $0.74 \pm 0.02 \mu\text{m}$ ), followed by  $\text{Al}_2\text{O}_3$  reinforced PMMA (Group 3,  $0.94 \pm 0.02 \mu\text{m}$ ),  $\text{ZrO}_2$  reinforced PMMA (Group 4,  $1.01 \pm 0.03 \mu\text{m}$ ), and unmodified 3D-printed PMMA (Group 2,  $1.06 \pm 0.02 \mu\text{m}$ ) showed the highest roughness.

## Discussion

The denture bases fabricated through 3D printing technology have proven to be better in comparison to their digital counterpart, the subtractive CAD CAM technique, in terms of cost effectiveness, reduced wastage, better detail reproduction and ability to print complex geometries.<sup>5,6</sup> However, the mechanical and surface properties of 3D printed denture bases are found to be inferior to both conventional and CAD CAM techniques.<sup>1,7,8</sup>

Several studies aimed at enhancing the properties of heat cured PMMA have stated that reinforcing PMMA with various fibres, and nanoparticles have significantly improved their physical, mechanical and surface properties. The most commonly used fibres for reinforcement are glass fibres, polyamide, polyethylene and polypropylene and natural fibres. The fillers included aluminium oxide, zirconium oxide, titanium oxide, silver, gold, platinum, palladium, silicon dioxide, hydroxyapatite, mica, and carbon in micro and nanosizes.<sup>9,10, 11, 12, 13, 14</sup>

This in-vitro study evaluated the flexural strength, surface hardness and surface roughness of unmodified 3D printed denture base PMMA resin and 2.5wt% Aluminium oxide and 1wt% Zirconium oxide nanoparticle reinforced 3D printed denture base PMMA resin and compared them with CAD CAM denture base PMMA resin. The specimens were tested for immediate mechanical and surface properties after 24-hour immersion in distilled water. To evaluate the long-term performance, the specimens were also tested for delayed properties after undergoing artificial aging to. To simulate the dynamic intraoral conditions, the specimens were immersed in artificial saliva for 30 days, followed by 5000 thermocycling cycles, which approximates six months of intraoral use.

Flexural strength represents the maximum stress a material can withstand before fracture under bending and is critical for denture durability. Consistent with earlier findings by Prpic et al<sup>7</sup>. and Gad et al.<sup>15</sup>, CAD CAM PMMA showed the highest strength due to dense pre-polymerization under high temperature and pressure, producing a cross-linked, low-porosity structure. The unmodified 3D printed PMMA recorded the lowest strength, attributable to incomplete polymerization and weak interlayer adhesion during additive fabrication.

Layer thickness, printing orientation, and post-curing directly influence mechanical outcomes, with thinner layers enhancing dimensional stability and polymerization.<sup>8,15</sup>

Reinforced 3D printed groups demonstrated improved flexural strength over unmodified PMMA. Al<sub>2</sub>O<sub>3</sub> reinforcement (2.5 wt%) significantly increased strength, consistent with Vojdani et al.<sup>16</sup>, who attributed the improvement to crack-deflection mechanisms of alumina fillers. SEM analysis in previous studies confirmed uniform Al<sub>2</sub>O<sub>3</sub> dispersion with minimal void formation at optimal concentrations, while excessive filler load (> 5 wt%) reduced strength due to agglomeration. Similarly, ZrO<sub>2</sub> reinforced PMMA (1 wt%) exhibited higher strength than both unmodified and Al<sub>2</sub>O<sub>3</sub> reinforced resins, aligning with Alshaikh et al.<sup>1</sup> and Azmy et al.<sup>17</sup>. This can be explained by ZrO<sub>2</sub>'s transformation from tetragonal to monoclinic phase, which absorbs crack-propagation energy and improves fracture resistance.

In the present study, the ZrO<sub>2</sub> group surpassed the Al<sub>2</sub>O<sub>3</sub> group for both immediate and delayed testing, demonstrating superior crack deflection and stability. Nevertheless, CAD CAM PMMA remained superior overall due to its pre-polymerized nature. Thermocycling decreased flexural strength in all groups owing to water-induced polymer degradation. The least deterioration occurred in the ZrO<sub>2</sub>-reinforced group, followed by Al<sub>2</sub>O<sub>3</sub>-reinforced, CAD CAM, and unmodified PMMA, indicating that nanoparticle reinforcement enhances resistance to thermal fatigue.

Surface hardness determines a material's resistance to wear and deformation. Low hardness can lead to surface abrasion, plaque retention, and color alteration, compromising longevity.<sup>1</sup> CAD CAM and heat-cured PMMA generally exhibit higher hardness than 3D printed PMMA, which has been attributed to material

composition, water sorption, layer thickness, and printing orientation.<sup>1,15</sup>

Incorporation of nanoparticles substantially enhanced hardness. In this study, CAD CAM PMMA showed the highest hardness, followed by ZrO<sub>2</sub> reinforced, Al<sub>2</sub>O<sub>3</sub> reinforced, and unmodified 3D printed PMMA. The difference between ZrO<sub>2</sub> and Al<sub>2</sub>O<sub>3</sub> groups was statistically significant. The intrinsic hardness of Al<sub>2</sub>O<sub>3</sub> is ≈15 GPa, which is lower than ZrO<sub>2</sub> which has a hardness of ≈20 GPa. This could explain the better results obtained by ZrO<sub>2</sub> in comparison to Al<sub>2</sub>O<sub>3</sub>. However, in agreement with previous studies,<sup>9,10,17,18</sup> the results confirm that both nanoparticles positively contribute to the improved surface hardness of 3D printed PMMA resin

Thermocycling significantly reduced surface hardness in all groups due to water absorption acting as a plasticizer within the PMMA matrix.<sup>1,15</sup> Among reinforced groups, Al<sub>2</sub>O<sub>3</sub> reinforced PMMA demonstrated better retention of hardness than ZrO<sub>2</sub> reinforced PMMA after aging. The improved stability of Al<sub>2</sub>O<sub>3</sub> may be attributed to its homogeneous dispersion and strong filler-matrix adhesion, which reduce filler debonding under stress. In contrast, phase transformation of ZrO<sub>2</sub> during thermal cycling can induce microstructural alterations that slightly compromise surface hardness

Surface roughness directly influences plaque accumulation, microbial colonization, and mucosal irritation. Highly polished denture surfaces are clinically desirable, as values above 2.2μm promote bacterial retention.<sup>9</sup> 3D printed PMMA typically shows greater surface roughness than CAD CAM PMMA due to its layer-by-layer structure and potential for incomplete interlayer fusion. Factors such as printing orientation, polishing technique, and resin composition also affect the final surface texture.<sup>1,5,9,15</sup>

In the present study, CAD CAM PMMA displayed the lowest roughness, followed by Al<sub>2</sub>O<sub>3</sub> reinforced, unmodified, and ZrO<sub>2</sub> -reinforced PMMA. The higher filler content and spherical morphology of Al<sub>2</sub>O<sub>3</sub> particles enhanced packing density and polishability, yielding smoother surfaces than ZrO<sub>2</sub>. Conversely, ZrO<sub>2</sub>'s angular particles resulted in slightly rougher surfaces.<sup>1,16</sup> Several authors<sup>1,9,17,19</sup> reported minimal or no increase in roughness at low nanoparticle concentrations.

After thermocycling, roughness increased in all groups due to water absorption and thermal expansion, which weaken polymer chain bonds and induce microcracks. Reinforced groups exhibited less degradation than unmodified PMMA, confirming the stabilizing effect of nanoparticles. Al<sub>2</sub>O<sub>3</sub> reinforcement showed the smallest increase ( $\Delta Ra = 0.03 \mu m$ ), whereas ZrO<sub>2</sub> displayed greater change ( $\Delta Ra = 0.08 \mu m$ ). The finer particle size and better interfacial bonding of Al<sub>2</sub>O<sub>3</sub> minimize filler debonding and matrix disruption, accounting for its smoother surface after aging.<sup>8,15</sup>

The present study has inherent limitations that must be acknowledged. The study did not replicate the anatomical configuration of a denture. The stress distribution of a denture in its anatomical form would be much more complex than that of the rectangular specimens tested in this study. Also, the specimens were only subjected to static forces; the dynamic loading that the dentures must withstand during intraoral use was not replicated in this in vitro study. The artificial aging only simulated 6 months of intraoral use; further studies simulating longer durations of intraoral use are recommended. The 3D printing of the test specimen was carried out in only one configuration; further studies with different printing orientations and layer thickness are recommended. The current study only evaluated the effect of Al<sub>2</sub>O<sub>3</sub> and ZrO<sub>2</sub>; the effect of other nanoparticles with varying

concentrations and the comparison between different nanoparticles should also be evaluated. Future studies should aim to overcome the aforementioned limitations to enhance the clinical relevance and applicability of the findings.

### **Clinical Implication**

Reinforcing 3D printed PMMA with zirconium oxide or aluminum oxide nanoparticles significantly increases its mechanical and surface properties, bringing its performance closer to CAD CAM PMMA. This suggests that modified 3D printed resins can be used as a potential alternative for definitive denture bases, offering improved durability and reduced fabrication cost.

### **Conclusion**

Within the limitations of this in-vitro study, it was concluded that:

- CAD-CAM PMMA exhibited the highest flexural strength and surface hardness, and the lowest surface roughness. However, a significant reduction in all three properties was observed on artificial aging.
- Unmodified 3D printed PMMA showed the least favourable results with the lowest flexural strength and surface hardness and highest surface roughness on both immediate and delayed testing.
- Reinforcement of 3D printed PMMA with 2.5 wt% Aluminium oxide significantly enhanced the immediate mechanical and surface properties. On delayed testing, Al<sub>2</sub>O<sub>3</sub> showed better resistance to deterioration of surface properties.
- Reinforcement of 3D printed PMMA with 1wt% Zirconium oxide significantly improved the immediate flexural strength, surface hardness and surface roughness. However, on delayed testing, significant reduction in both mechanical and surface properties were observed.
- CAD-CAM PMMA exhibited the highest mechanical and surface properties, while unmodified 3D printed

PMMA presented the lowest values. However, reinforcing 3D printed PMMA with zirconium oxide significantly improved the immediate and delayed flexural strength, while aluminium oxide reinforcement exhibited significantly lower surface roughness and is better suited to resist surface degradation caused by thermal stresses.

In conclusion, nanoparticle reinforcement has proven to be a promising strategy to improve the mechanical and surface properties of 3D printed PMMA. However, this study has revealed that the choice of nanoparticles should be guided by the property that needs to be enhanced, as no single nanoparticle is capable of imparting all the desired properties.

#### References

1. Alshaikh AA, Khattar A, Almindil IA, Alsaif MH, Akhtar S, Khan SQ, Gad MM. 3Dprinted nanocomposite denture-base resins: effect of ZrO<sub>2</sub> nanoparticles on the mechanical and surface properties in vitro. *Nanomaterials*. 2022 Jul 18;12(14):2451.
2. Lee DJ, Saponaro PC. Management of edentulous patients. *Dental Clinics*. 2019 Apr 1;63(2):249-61.
3. Alqutaibi AY, Baik A, Almuzaini SA, Farghal AE, Alnazzawi AA, Borzangy S, Aboalrejal AN, AbdElaziz MH, Mahmoud II, Zafar MS. Polymeric denture base materials: A review. *Polymers*. 2023 Jul 31;15(15):3258.
4. Davidowitz G, Kotick PG. The use of CAD/CAM in dentistry. *Dental Clinics of North America*. 2011 Jul;55(3):559-ix
5. Souza LF, Pires TS, Kist PP, Valandro LF, Moraes RR, Özcan M, Pereira GK. 3D printed, subtractive, and conventional acrylic resins: Evaluation of monotonic versus fatigue behavior and surface characteristics. *Journal of the Mechanical Behavior of Biomedical Materials*. 2024 Jul 1;155:106556.
6. Majeed HF, Hamad TI, Bairam LR. Enhancing 3D-printed denture base resins: A review of material innovations. *Science Progress*. 2024 Jul;107(3):00368504241263484.
7. Prpić V, Schauerl Z, Čatić A, Dulčić N, Čimić S. Comparison of mechanical properties of 3D-printed, CAD/CAM, and conventional denture base materials. *Journal of Prosthodontics*. 2020 Jul;29(6):524-8.
8. Temizci T, Bozoğulları HN. Effect of thermal cycling on the flexural strength of 3-D printed, CAD/CAM milled and heat-polymerized denture base materials. *BMC Oral Health*. 2024 Mar 20;24(1):357.
9. Vojdani M, Bagheri R, Khaledi AA. Effects of aluminum oxide addition on the flexural strength, surface hardness, and roughness of heat-polymerized acrylic resin. *Journal of Dental Sciences*. 2012 Sep 1;7(3):238-44.
10. Ahmed MA, Ebrahim MI. Effect of zirconium oxide nano-fillers addition on the flexural strength, fracture toughness, and hardness of heat-polymerized acrylic resin. *World Journal of Nano Science and Engineering*. 2014 May 9;4(2):50-7.
11. Jagger DC, Harrison A, Jandt KD. The reinforcement of dentures. *Journal of Oral Rehabilitation*. 1999 Mar;26(3):185-94.
12. Gad MM, Fouda SM, Al-Harbi FA, Näpänkangas R, Raustia A. PMMA denture base material enhancement: a review of fiber, filler, and nanofiller addition. *International Journal of Nanomedicine*. 2017 May 17:3801-12.
13. Dhole RI, Srivatsa G, Shetty R, Huddar D, Sankeshwari B, Chopade S. Reinforcement of aluminum oxide filler on the flexural strength of

different types of denture base resins: An in vitro study. *Journal of Clinical and Diagnostic Research: JCDR*. 2017 Apr 1;11(4):ZC101

14. Alrahlah A, Fouad H, Hashem M, Niazy AA, AlBadah A. Titanium oxide (TiO<sub>2</sub>)/polymethylmethacrylate (PMMA) denture base nanocomposites: mechanical, viscoelastic and antibacterial behavior. *Materials*. 2018 Jun 27;11(7):1096.
15. Gad MM, Fouda SM, Abualsaud R, Alshahrani FA, Al-Thobity AM, Khan SQ, Akhtar S, Ateeq IS, Helal MA, Al-Harbi FA. Strength and surface properties of a 3D-printed denture base polymer. *Journal of Prosthodontics*. 2022 Jun;31(5):412-8.
16. Geerts GA, Jooste CH. A comparison of the bond strengths of microwave-and water bath-cured denture material. *The Journal of Prosthetic Dentistry*. 1993 Nov 1;70(5):406-9.
17. Azmy E, Al-Kholy MR, Al-Thobity AM, Gad MM, Helal MA. Comparative effect of incorporation of ZrO<sub>2</sub>, TiO<sub>2</sub>, and SiO<sub>2</sub> nanoparticles on the strength and surface properties of PMMA denture base material: an in vitro study. *International Journal of Biomaterials*. 2022;2022(1):5856545
18. Alhotan A, Yates J, Zidan S, Haider J, Silikas N. Flexural strength and hardness of filler-reinforced PMMA targeted for denture base application. *Materials*. 2021 May 19;14(10):2659.
19. Khattar A, Alghafli JA, Muheef MA, Alsalem AM, Al-Dubays MA, AlHussain HM, AlShoalah HM, Khan SQ, AlEraky DM, Gad MM. Antibiofilm activity of 3D-printed nanocomposite resin: impact of ZrO<sub>2</sub> nanoparticles. *Nanomaterials*. 2023 Feb 1;13(3):59.